# Study of the dielectric response in mineral oil using frequency-domain measurement

Yuan Zhou, Miao Hao, George Chen, Gordon Wilson, and Paul Jarman

Citation: Journal of Applied Physics **115**, 124105 (2014); doi: 10.1063/1.4869546
View online: http://dx.doi.org/10.1063/1.4869546
View Table of Contents: http://scitation.aip.org/content/aip/journal/jap/115/12?ver=pdfcov
Published by the AIP Publishing

# Study of the dielectric response in mineral oil using frequency-domain measurement

Yuan Zhou,[1] Miao Hao,[1] George Chen,[1] Gordon Wilson,[2] and Paul Jarman[2]
[1]*University of Southampton, Highfield Campus, Southampton SO17 1BJ, United Kingdom*
[2]*National Grid UK, Warwick, United Kingdom*

(Received 4 January 2014; accepted 14 March 2014; published online 27 March 2014)

Dielectric spectroscopy is a powerful tool to study dipole relaxation, electrical conduction, and structure of molecules. Electrode polarization, as a parasitic effect due to the blocking of charge carriers in the vicinity of an electrode, can make the frequency response at low frequency difficult to understand. Since charge carriers in mineral oil are not only generated from dissociation but also from injection at electrodes, current induced by motion of injected charge carriers should also be taken into consideration. The polarization caused by the injection current has been studied in this paper. When the electric field is not intense, the injection current is proportional to the field and only contributes to the imaginary part of the complex permittivity. A new model has been proposed with this injection current being involved. The frequency responses of three different kinds of mineral oils have been measured and this new polarization model has been used to fit the experimental data. According to the simulation result, the frequency-dependent curves of complex dielectric permittivity calculated from the polarization model could fit the experimental data well. The amount of the injected charge carriers increases with the aging time. This new model enables one to gain a better understanding of electrical conduction in mineral oil. © *2014 AIP Publishing LLC*.
[http://dx.doi.org/10.1063/1.4869546]

## I. INTRODUCTION

Starting in the late nineteenth century, dielectric spectroscopy techniques were developed for measuring polarization of various materials. Nowadays, a typical measurement can cover an extensive range of frequency from several GHz to micro-Hz. It is a powerful tool to study dipole relaxation, electrical conduction, structure of molecules, etc.[1] This frequency-domain method has been used to investigate dielectric properties of mineral oil and to estimate the remaining life period of a transformer in service.[2–6] Parameters obtained from this frequency-domain method have a good capability for determination of physical and chemical properties of insulating oil.[2–8]

It is generally accepted that the electrode effect is a parasitic effect during dielectric spectroscopy measurement, since it can be added to the real dielectric response and make experimental result difficult to understand.[1] This effect originates from the blocking of charge carriers at the liquid/solid interface. If the charge carriers are blocked by the electrode, the accumulation of charge carriers in the vicinity of the electrode could lead to a non-homogeneous electric field distribution and a reduction of the total current. The presence of space charge can result in a significant increase of the real part of complex permittivity when the frequency is low.[1] The space charge polarization has been studied both theoretically and experimentally by many researchers.[9–29] Jaffe has presented a general solution to the polarization under a homogeneous field or a hyperbolic field and his theory has been verified in both electrolytic solutions and dielectric liquid.[9–13] Macdonald and Friauf have obtained more general solutions based on the Jaffe's studies, and their theoretical space charge polarization expressions have been accepted and used to analysing the frequency response result that is measured from experiments.[14–20] Coelho has proposed a model by taking into account the combined influence of field and thermal diffusion.[21,22] Frood and Gallagher have applied Coelho's model in liquid sample and reported that Coelho's model was unable to explain the behaviour of the imaginary part of the complex permittivity.[23] Frood and Gallagher thought there might be highly mobile charge carriers in liquid.[23] Methods used previously lead to non-linear solutions are based on linear approximations that is valid for low voltages only; thus, Stern and Weaver provided a computer-based method to calculate the effective complex permittivity of a solid dielectric material under high electric field.[24] Sawada has studied the space charge polarization based on computer simulation and indicated that the presence of the space charge might have an adverse impact on Macdonald's frequency response theory.[25–29]

As shown in the literatures that have been published, the frequency responses of mineral oil share several common features.[2–8] The real part of the complex permittivity would increase when the frequency decreases, whilst the imaginary part decreases with frequency with a slope close to −1 in a log-log scale.[2–8] However, the curves of the imaginary part of the complex permittivity which is calculated from current theories can reach a peak value and then start to decrease as the frequency decreases, which is against the experimental data.[2–6,9–29] Therefore, there should be other charge transportation processes being involved. In this paper, this new type of charge carriers is assumed to be the injected charge carriers and these injected charge carriers are assumed to be charged in the region close to one electrode and discharged in the vicinity of the opposite electrode. In nonpolar liquids,

 

charge injection and transportation are different from that in solid and gas. The charge injection may be described by a two-step process: the charge carriers will be created at the electrodes, and then extracted by the electric field from the image force region.[30,31] The second step has been fully understood, whilst the mechanism of charge transfer at electrodes is still not clear.[30] The charge injection in liquid was first studied by Felici in 1978.[32] Felici took into account the field distribution in the region that was close to the metal/liquid interface and the charge transportation mechanisms participating in a region near the interface and derived an analytic solution for charge injection.[32] Later, Denat *et al.* have studied the electrical conduction of liquids when injection and dissociation are both present.[33–36] This ionic injection theory has been widely studied and verified in various kinds of the liquid under different experimental conditions.[30–41] Alj *et al.* analysed the experimental data based on this injection theory and they have found a strong correlation between the current that is contributed by injection and the concentration of ions at thermodynamic equilibrium.[30] Nemamcha verified this ionic injection equations under different temperatures and found out the field dependence of the injected current density followed the Felici's theory regardless the temperature.[31] Pontiga and Castellanos suggested that Onsager's theory for the dissociation of ionic pairs in the bulk should be added to the injection theory.[40–42]

As charge injection can contribute to the total conductivity, the current induced from injection should also be taken into consideration in analysing of frequency response in mineral oil. In our previous work, an ohmic component has been added to the classic ionic drift and diffusion model and this new model can fit the experimental data quite well.[43] In this paper, the dielectric characteristics of three types of mineral oils with different aging times are studied using dielectric spectroscopy method. The polarization caused by the injection is studied for the following two cases: (A) the charge carriers that are created at one electrode can get to the opposite electrode in a full cycle; and (B) these charge carriers are unable to travel to the opposite electrode. A new charge drift and diffusion model is proposed and the parameters used in the numerical calculation are compared.

## II. GENERAL EQUATIONS FOR FREQUENCY RESPONSE IN MINERAL OIL

Let us consider a parallel electrode system filled up with mineral oil. Here, we assume that diffusion coefficient, mobility, density, and charge that is a single charge carrier carried of positive ions are equal to those of negative ions; therefore, the density of positive charge carriers and negative charge carriers can be written as

$$n_+ = n_- = n_0 = \sigma/q(\mu_+ + \mu_-), \tag{1}$$

where $n_+$ and $n_-$ are the density for the positive charge carriers and the negative charge carriers, $\sigma$ is the conductivity of the mineral oil, $q$ is the charge carried by a single charge carrier, and $\mu_+$ and $\mu_-$ are the mobility for the positive and negative charge carriers, respectively.

There are three forces acting upon the charge carriers. The Coulomb force, the friction force, and the force from the pressure of other ions can affect the velocity of the charge carriers. The motion of the charge carriers and the time needed for the ion to reach its limit velocity in the liquid has been well studied.[44,45] The velocity of the charge carriers can be safely assumed to be proportional to the field if the frequency is below 100 Hz and the field is not high. Thus, the velocity can be described as

$$\vec{v} = \mu\vec{E}, \tag{2}$$

in which $\vec{v}$ is the velocity, $\vec{E}$ is the field, and $\mu$ is the mobility.

Due to the presence of the space charge, the electric field is subject to the Poisson equation

$$\frac{\partial E(x,t)}{\partial x} = q[n_+(x,t) - n_-(x,t)]/\varepsilon_0\varepsilon_r, \tag{3}$$

where $\varepsilon_0$ is the dielectric constant of vacuum and $\varepsilon_r$ is the relative dielectric constant of the liquid. If the electric potential between these two electrodes is $V(t)$ and the distance between them is $l$, the electric field should obey the following equation:

$$V(t) = \int_0^l E(x,t)dx. \tag{4}$$

If charge carriers are assumed to being continuously generated from the dissociation of ionic pairs and ionic pairs are formed by the recombination of these charge carriers conversely, this dissociation and recombination process can be described using

$$\frac{dn_+}{dt} = \frac{dn_-}{dt} = K_d c - K_r n_+ n_-, \tag{5}$$

where $c$ is the concentration of ionic pairs, $K_d$ is the dissociation constant, and $K_r$ is the recombination constant. The recombination constant can be written as[46]

$$K_r = q\frac{\mu_+ + \mu_-}{\varepsilon_0\varepsilon_r}. \tag{6}$$

The dissociation constant can be calculated from Eq. (5) by assuming the steady state equilibrium has been reached in the mineral oil

$$K_d = K_r n_+ n_-/c = K_r {n_0}^2/c. \tag{7}$$

When the flow of oil can be ignored, the density of positive and negative charge carriers can be denoted as

$$\frac{dn_+(x,t)}{dt} = K_r n_0^2 - K_r n_+(x,t)n_-(x,t) + D_+\frac{\partial^2 n_+(x,t)}{\partial x^2} - \mu_+\frac{\partial[n_+(x,t)E(x,t)]}{\partial x}, \tag{8}$$

$$\frac{dn_-(x,t)}{dt} = K_r n_0^2 - K_r n_+(x,t)n_-(x,t) + D_-\frac{\partial^2 n_-(x,t)}{\partial x^2} + \mu_-\frac{\partial[n_-(x,t)E(x,t)]}{\partial x}, \tag{9}$$

where $D$ is the diffusion coefficient. According to Einstein relation, the diffusion rate can be written as

$$D_{\pm} = \frac{\mu_{\pm} k_b T}{q}, \tag{10}$$

where $k_b$ is the Boltzmann constant and $T$ is the absolute temperature. If both electrodes are completely blocked electrodes and no current arising from the motion of either type of ions flow across the electrodes, the boundary conditions at $x = 0$ and $x = l$ can be described as

$$D_{\pm} \frac{\partial n_{\pm}(0,t)}{\partial x} - \mu_{\pm} n_{\pm}(0,t) E(0,t) = 0, \tag{11}$$

$$D_{\pm} \frac{\partial n_{\pm}(l,t)}{\partial x} - \mu_{\pm} n_{\pm}(l,t) E(l,t) = 0. \tag{12}$$

In the system, positive or negative charges should be supplied to the electrodes by the power source and become bound charges to compensate the charge carriers that approach the electrodes, so that the voltage between the two electrodes can be equal to the output voltage from the power source. Because there is no charge exchange at the interface, the current flows through the measuring circuit can be calculated from the change of these bounded charges. The quantity of these bounded charges at the electrode at $x = l$ can be written as

$$Q(t) = -\frac{q}{l} \int_0^l x[n_+(x,t) - n_-(x,t)]dx. \tag{13}$$

Thus, the total current $J_c(t)$ that was caused by the motion of the charge carriers can be denoted as

$$J_c(t) = -dQ(t)/dt. \tag{14}$$

When one material does not contain any mobile charge carriers, its permittivity consists of the contribution of electronic, atomic and dipole polarizations. As pointed out by Sawada, the permittivity contributed by electronic, atomic, and dipole polarizations can be assumed to be constant within the frequency range of the space charge polarization studied and the dielectric loss brought about by these polarizations is negligible.[25–27] Thus, when the external electric potential that was applied upon these two electrodes is a sinusoidal voltage $V(t) = V_0 \sin(\omega t)$, the relative dielectric permittivity involves the electrode polarization can be written as

$$\begin{cases} \varepsilon''(\omega) = \dfrac{2 I_{real} l}{\varepsilon_0 \omega V_0 S} \\ \varepsilon'(\omega) = \dfrac{2 I_{imag} l}{\varepsilon_0 \omega V_0 S} + \varepsilon_s, \end{cases} \tag{15}$$

with

$$\begin{cases} I_{real} = f \displaystyle\int_0^{1/f} J_c(t) S \sin(\omega t) dt \\ I_{imag} = f \displaystyle\int_0^{1/f} J_c(t) S \cos(\omega t) dt, \end{cases} \tag{16}$$

where $f$ is the frequency, $S$ is the surface area of the electrode, and $\omega$ is the angular frequency. $\varepsilon_s$ is the dielectric constant of the material consisting of the contributions of electronic, atomic, and dipole polarizations, $I_{real}$ is the integration of the current that contributes to the imaginary part of the complex permittivity, while $I_{imag}$ is the integration of the current that can affect the real part of the complex permittivity.

The injection of charge carriers can be described by means of a two-step process: (A) charge carriers are created at a region that is close to the metal/liquid interface; (B) these newly generated charge carriers are extracted from that region and drift into the bulk. The rate of extraction of these injected charge carriers is determined by two transport mechanisms: ionic migration and diffusion. Felici has studied the injection in insulating hydrocarbon liquid and obtained an analytical solution[32,33]

$$q_i = q_0 \times \exp\left(-\frac{e^2}{16\pi\varepsilon_0\varepsilon_r x_B k_b T}\right) \Big/ (2b \times K_1(2b)), \tag{17}$$

with

$$b = \sqrt{(e^3 E / 16\pi\varepsilon_0\varepsilon_r k_b{}^2 T^2)}, \tag{18}$$

where $q_i$ is the charge density that is considerable far away from the electrode, $x_B$ is the minimum approach of a charge carrier to the metal electrode, $q_0$ is the charge density at $x_B$, and $K_1$ is the modified Hankel function. Here, we assume there are only one kind of injected charge carriers in the mineral oil and these injected charge carriers are positive charge carriers. Thus, there will be no recombination for the injected charge carries. If the extraction rate is far lower than the injection rate at the electrode, the field dependence of the injection current density can be denoted as[30,31]

$$j_i = q_i \mu_i E = q_i^0 \mu_i E / [2b \times K_1(2b)], \tag{19}$$

where $q_i^0$ a constant charge density that depends on the nature of liquid and electrode and $\mu_i$ is the mobility of these injected charge carriers. When the field is not very high, $2bK_1(2b) \approx 1$. At a low electric field of 2V/mm, this injection process can be safely assumed to be autonomous.[40,41,45]

If the diffusion effect can be ignored in the analysis of the injection current in dielectric liquid, and the internal field can be treated as a homogeneous field, the time dependent injected current density $j_i(t)$ that is in the vicinity of the electrode can be described as

$$j_i(t) = q_i^0 \mu_i E(t) / [2b \times K_1(2b)] \approx q_i^0 \mu_i E(t), \tag{20}$$

in which $\mu_i$ is the mobility of the injected charge carriers. Since the total injection current is caused by the motion of all the injected charge carriers. The total current density $J_i(t)$ that is from the injection can be denoted as

$$J_i(t) = \frac{1}{l} \int_0^l j_i(x,t) dt = \mu_i E(t) \rho(t) / l, \tag{21}$$

where $\rho(t)$ is the total injected charge and $l$ is the distance between two electrodes. There are two different cases for the

polarization caused by the injection. First, the injected charge carriers created at one electrode are unable to reach the opposite electrode in a full cycle. Second, these injected charge carriers can get to the opposite electrode in a full cycle.

First, we will discuss the polarization under the condition that the charge carriers cannot reach the opposite electrodes in a cycle.

If the charge carriers can be neutralized immediately once they approach the oil/metal interface, the total injected charge can be calculated using the following expression:

$$\rho(t_0) = \int_0^{t_0} j_i(t)dt = \int_0^{t_0} q_i^0 \mu_i E(t)dt. \tag{22}$$

When the external voltage applied to the electrodes is $V(t) = V_0 \sin(\omega t)$, we can get

$$\rho(t_0) = \int_0^{t_0} q_i^0 \mu_i (V_0/l)\sin(\omega t)dt = \frac{q_i^0 \mu_i V_0}{\omega l}[1 - \cos(\omega t_0)]. \tag{23}$$

On considering that the injection can also take place at the opposite electrode, the current that was injected from the opposite electrode can be denoted simply as

$$\rho_{oppo}(t_0) = \frac{q_i^0 \mu_i V_0}{\omega l}[1 + \cos(\omega t_0)], \tag{24}$$

in which $\rho_{oppo}(t_0)$ is the total charge that was injected from the opposite electrode. Therefore, the total charge $\rho_{tot}(t_0)$ injected from both electrodes should be

$$\rho_{tot}(t_0) = \left[\rho(t_0) + \rho_{oppo}(t_0)\right] = \frac{2q_i^0 \mu_i V_0}{\omega l}, \tag{25}$$

which means that $\rho_{tot}$ is constant value and can only be determined by the frequency. Thus, the total injection current from both two electrodes is

$$J_i(t) = \mu_i V(t)\rho_{tot}(t)/l^2 = \frac{2q_i^0 \mu_i^2 V_0^2}{\omega l^3}[\sin(\omega t)]. \tag{26}$$

After using Eq. (16), we can obtain

$$\begin{cases} \Delta I_{real} = \dfrac{1}{T}\displaystyle\int_0^T \frac{2q_i^0 {\mu_i}^2 {V_0}^2}{\omega l^3}[\sin^2(\omega t)]Sdt = \frac{q_i^0 {\mu_i}^2 {V_0}^2 S}{\omega l^3} \\ \Delta I_{imag} = \dfrac{1}{T}\displaystyle\int_0^T \frac{2q_i^0 {\mu_i}^2 {V_0}^2}{\omega l^3}\sin(\omega t)\cos(\omega t)Sdt = 0. \end{cases} \tag{27}$$

By substituting Eq. (27) into Eq. (15), the polarization caused by the injection can be denoted as

$$\begin{cases} \Delta\varepsilon'' = \dfrac{2\Delta I_{real}}{\varepsilon_0 \omega E_0 S} = \dfrac{2q_i^0 {\mu_i}^2 V_0}{\varepsilon_0 \omega^2 l^2} \\ \Delta\varepsilon' = 0, \end{cases} \tag{28}$$

in which $\Delta I_{real}$ and $\Delta I_{imag}$ are the integration of the total current that is only contributed by the injection current, whilst $\Delta\varepsilon''$ and $\Delta\varepsilon'$ are the changes of the complex permittivity in imaginary part and real part, respectively. However, it seems that the imaginary part will decrease faster as the frequency increases, which is not in a good agreement with our experimental result.[43]

If $\mu_i > \omega l^2/2V_0$, the injected charge carriers are fast enough to reach the opposite electrode. Here, we assume that the injected charge carriers can be also neutralized immediately when they can get close to the electrode and the internal field does not change a lot and can be treated as a homogenous field. A sinusoidal field with magnitude $V_0$ and period $T$ is shown in Fig. 1. If the injection takes places at $t = 0$ at one electrode, for the other electrode the charge injection starts at $t = T/2$. In the following paragraphs, we will refer the electrode at which that injection begins at $t = 0$ as the first electrode and the other electrode as the second electrode for simplicity.

For the first electrode, the injected current density in the vicinity of this electrode can be denoted as

$$\begin{cases} j_i = q_i^0 \mu_i (V_0/l)\sin(\omega t) & (0 < t < T/2) \\ j_i = 0 & (T/2 < t < T). \end{cases} \tag{29}$$

The total charge that injected from the first electrode from *t1* to *t2* under the circumstance that the charge carriers that injected from the first electrode at *t1* can just reach the second electrode at *t2* can be written as

$$\rho_1(t2) = \int_{t1}^{t2} j_i(t)dt = q_i^0 \int_{t1}^{t2} \mu_i (V_0/l)\sin(\omega t)dt. \tag{30}$$

The distance between the two electrodes, $l$, also satisfies

$$l = \int_{t1}^{t2} \mu_i (V_0/l)\sin(\omega t)dt. \tag{31}$$

Therefore, the total amount of charge that was injected from the first electrode at $t = t2$ can be denoted as

$$\rho_1(t2) = q_i^0 l. \tag{32}$$

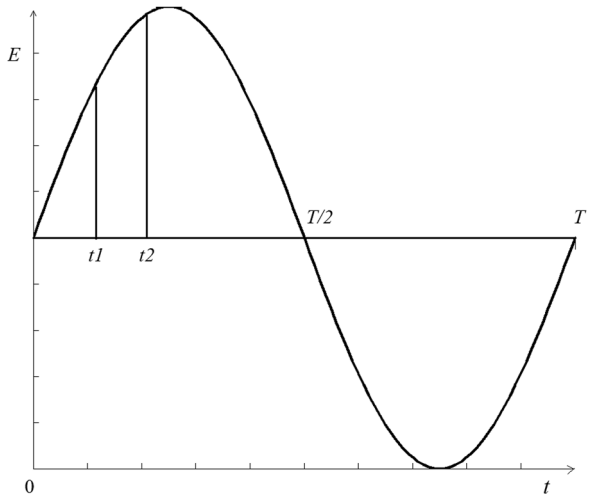


FIG. 1. A sinusoidal electric field with magnitude $E_0$ and period $T$.

At the very beginning, the injected charge carriers do not have enough time to reach the second electrode and the minimum time required for the charge carriers that are injected at $t=0$ can get to the second electrode is $t_{\min} = \arccos(1 - \omega l^2/\mu V_0)$.

Thus, the total charge that injected from the first electrode at the beginning is

$$\rho_1(t_0) = \int_0^{t_0} q_i^0 \mu_i (V_0/l)\sin(\omega t)dt = \frac{q_i^0 \mu_i V_0}{\omega l}(1-\cos(\omega t_0)) \quad (0 < t_0 < t_{\min}). \tag{33}$$

When $T/2 > t > t_{\min}$, as the charge carriers that was injected from the first electrode can reach the second electrode, Eq. (31) can be used to calculate the total charge that was injected from the first electrode and the amount of these injected charge can be denoted as

$$\rho_1(t) = q_i^0 l \quad (T/2 > t > t_{\min}). \tag{34}$$

When the electric field reverses at $t=T/2$, the total injected charge from the first electrode can be simply obtained as $\rho_1(T/2) = q_i^0 l$. After the field reverse, the injected charge carriers will start to be neutralized at the electrode from which they are injected. Therefore, the total amount of charge after the field reverse can be written as

$$\rho_1(t) = q_i^0 l + \int_{T/2}^{T/2+t_{\min}} q_i^0 \mu_i (V(t)/l)dt = q_i^0 l - \frac{q_i^0 \mu_i V_0}{\omega l}(1+\cos(\omega t)) \quad (T/2 < t < T/2 + t_{\min}). \tag{35}$$

After all these charge carriers have been extracted, the current will be zero.

To sum up, the total charge due to the injection from the first electrode in a full field cycle can be denoted as

$$\begin{cases} \rho_1(t) = \dfrac{q_i^0 \mu_i V_0}{\omega l}(1-\cos(\omega t)) & (0 < t < t_{\min}) \\ = q_i^0 l & (t_{\min} < t < T/2) \\ = q_i^0 l - \dfrac{q_i^0 \mu_i V_0}{\omega l}(1+\cos(\omega t)) & (T/2 < t < T/2 + t_{\min}) \\ = 0 & (T/2 + t_{\min} < t < T). \end{cases} \tag{36}$$

For the second electrode, we can do the same analysis. Easily, we can get

$$\begin{cases} \rho_{oppo}(t) = q_i^0 l - \dfrac{q_i^0 \mu V_0}{\omega l}(1-\cos(\omega t)) & (0 < t < t_{\min}) \\ = 0 & (t_{\min} < t < T/2) \\ = \dfrac{q_i^0 \mu V_0}{\omega l}(1+\cos(\omega t)) & (T/2 < t < T/2 + t_{\min}) \\ = q_i^0 l & (T/2 + t_{\min} < t < T). \end{cases} \tag{37}$$

Therefore, in a full circle, we can always get

$$\rho_{tot}(t) = \rho_1(t) + \rho_{oppo}(t) = q_i^0 l. \tag{38}$$

Thus, the total injected charge is constant in the bulk in a full cycle, and it no longer depends on the frequency.

The total current from injection is

$$J_i(t) = \mu_i V(t) \rho_{tot}(t)/l^2 = q_i^0 \mu_i (V_0/l)\sin(\omega t). \tag{39}$$

By substituting Eq. (39) into Eqs. (15) and (16), we can get

$$\begin{cases} \Delta\varepsilon'' = \dfrac{q_i^0 \mu_i}{\omega \varepsilon_0}. \\ \Delta\varepsilon' = 0 \end{cases} \tag{40}$$

Thus, the polarization caused by the injection becomes

$$\begin{cases} \Delta\varepsilon' = 0 \\ \Delta\varepsilon'' = \dfrac{q_i^0 \mu_i}{\omega \varepsilon_0} \times \dfrac{2\mu_i V_0}{\omega l^2} & (2\mu_i V_0/\omega l^2 < 1) \\ \Delta\varepsilon'' = \dfrac{q_i^0 \mu_i}{\omega \varepsilon_0} & (2\mu_i V_0/\omega l^2 > 1). \end{cases} \tag{41}$$

Adding Eq. (41) to Eqs. (15) and (16), the relative dielectric permittivity involves the polarization from the injection can be written as

$$\begin{cases} \varepsilon'(\omega) = \dfrac{2I_{imag} l}{\varepsilon_0 \omega V_0 S} + \varepsilon_s \\ \varepsilon''(\omega) = \dfrac{2I_{real} l}{\varepsilon_0 \omega V_0 S} + \dfrac{q_i^0 \mu_i}{\omega \varepsilon_0} \times \dfrac{2\mu_i V_0}{\omega l^2} & (2\mu_i V_0/\omega l^2 < 1) \\ \varepsilon''(\omega) = \dfrac{2I_{real} l}{\varepsilon_0 \omega V_0 S} + \dfrac{q_i^0 \mu_i}{\omega \varepsilon_0} & (2\mu_i V_0/\omega l^2 > 1), \end{cases} \tag{42}$$

with

$$\begin{cases} I_{real} = f\int_0^{1/f} J_c(t) S \sin(\omega t)dt \\ I_{imag} = f\int_0^{1/f} J_c(t) S \cos(\omega t)dt. \end{cases} \tag{43}$$

## III. COMPARISON BETWEEN EXPERIMENT AND THEORY

The frequency-domain measurements were preceded using a Solartron 1296 dielectric interface and model 1260A impedance/-gain phase analyser. The oil sample was vacuumed for half an hour to remove dissolved gas. The voltage across the sample was 1 V and the gap between two electrodes was 0.5 mm. The experiments were carried out at four different temperatures (25 °C, 50 °C, 75 °C, and 90 °C). The test cell filled with oil was maintained at the desired temperature for at least half an hour before each measurement. The frequency range for the test is 100 Hz–0.01 Hz. Here, the

frequency responses of three different types of mineral oil: the fresh oil, lightly aged oil (aged 10 years), and heavily aged oil (aged over 50 years), have been measured and compared.

Figures 2–7 show the results of the frequency response of the oil samples, which were measured at different temperatures. As shown in Figures 2–4, the real parts of the relative complex permittivity of the all three kinds of mineral oil are around 2.1–2.4 in frequency ranges from 1 Hz to 100 Hz and they seem to be constant regardless of the conductivity. The space charge polarization can be clearly observed in the form of the increase of the real part of the complex permittivity at low frequency. This result indicates that the space charge polarization plays a dominant role in the frequency response when the frequency is below 1 Hz. As mineral oil is aged, more charge carriers will be generated. Since there are more charge carriers, the space charge polarization should become more significant and a higher real part of the complex permittivity can be observed. The imaginary part of the complex permittivity decreases linearly with slope of −1 in log-log scale; thus, the mechanism of the electric conduction does not change remarkably in the frequency range studied (100 Hz–0.01 Hz). The imaginary part of the complex permittivity that was calculated based on current theory of space charge polarization can reach a peak and then start to decrease as the frequency decreases.[9–29] However, the observation in Figures 4–7 shows that the imaginary part of the complex permittivity virtually decreases with frequency with slope of −1 over the whole frequency range that was studied in this paper and it indicates a near-constant conductivity of the mineral oil. This inconsistence has been attributed to a low density of highly mobile charge carriers arising from charge injection at the electrodes.[23] The temperature dependences of the complex permittivity are also depicted in Figures 2–7. The shifting of the curves towards higher frequencies can be observed as the dissociation rate and the mobility of the charge carriers will increase when the temperature becomes higher.

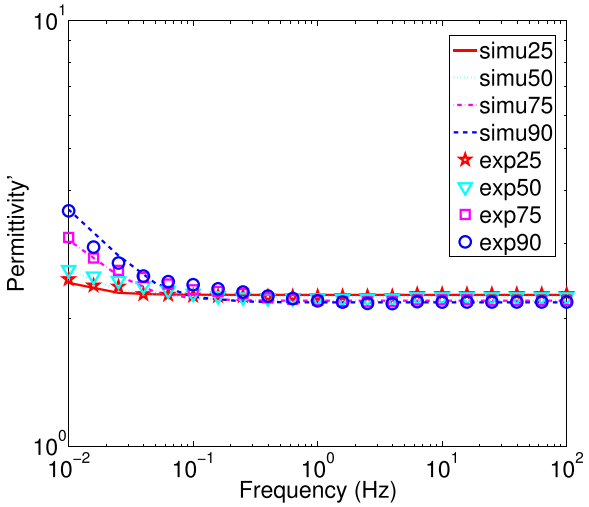


FIG. 3. The simulation and experimental result of the real part of the complex permittivity of the lightly aged oil. Dashed line, dashed-dotted line, dotted line, and solid line are calculated by the means of the curve fitting at 90 °C, 75 °C, 50 °C, and 25 °C, respectively. Circular markers, square markers, triangular markers, and pentacle markers represent the observed value at 90 °C, 75 °C, 50 °C, and 25 °C, respectively.

Similar to the author's previous study, we assume that there are two kinds of charge carriers in our charge transportation model, the first kind is mainly dissociated from the ionic pairs and can be fully blocked by the metal electrode, whilst the second kind can be charged from one electrode and discharged at the opposite electrode. We have defined a parameter, $\alpha$, the ratio of the conductivity that contributed from the injection over the total conductivity. This ratio is defined as

$$\alpha = \sigma_i/\sigma, \tag{44}$$

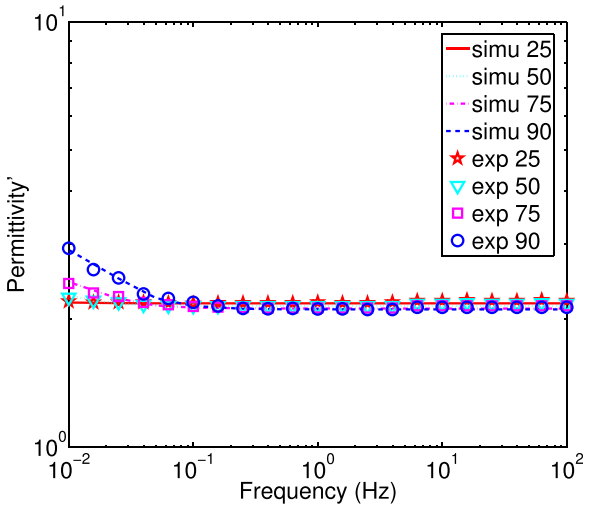


FIG. 2. The simulation and experimental result of the real part of the complex permittivity of the fresh oil. Dashed line, dashed-dotted line, dotted line, and solid line are calculated by the means of the curve fitting at 90 °C, 75 °C, 50 °C, and 25 °C, respectively. Circular markers, square markers, triangular markers, and pentacle markers represent the observed value at 90 °C, 75 °C, 50 °C, and 25 °C, respectively.

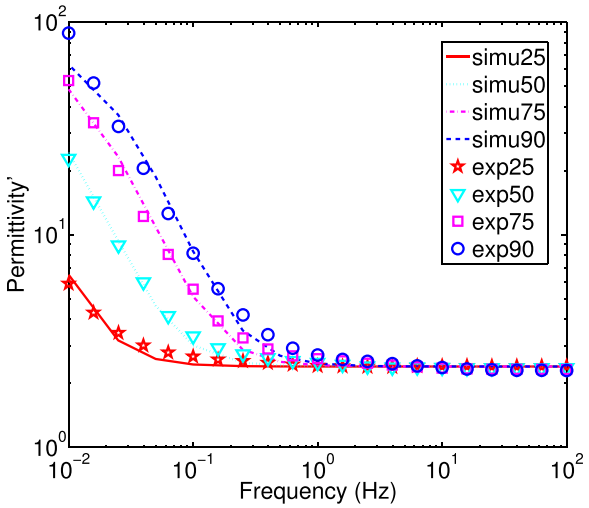


FIG. 4. The simulation and experimental result of the real part of the complex permittivity of the heavily aged oil. Dashed line, dashed-dotted line, dotted line, and solid line are calculated by the means of the curve fitting at 90 °C, 75 °C, 50 °C, and 25 °C, respectively. Circular markers, square markers, triangular markers, and pentacle markers represent the observed value at 90 °C, 75 °C, 50 °C, and 25 °C, respectively.

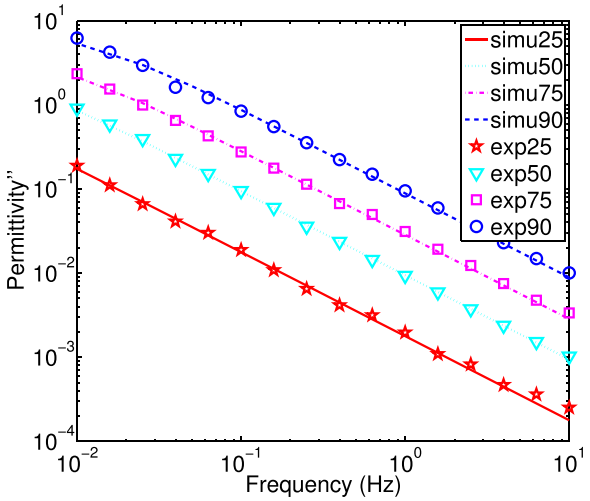


FIG. 5. The simulation and experimental result of the imaginary part of the complex permittivity of the fresh oil. Dashed line, dashed-dotted line, dotted line, and solid line are calculated by the means of the curve fitting at 90 °C, 75 °C, 50 °C, and 25 °C, respectively. Circular markers, square markers, triangular markers, and pentacle markers represent the observed value at 90 °C, 75 °C, 50 °C, and 25 °C, respectively.

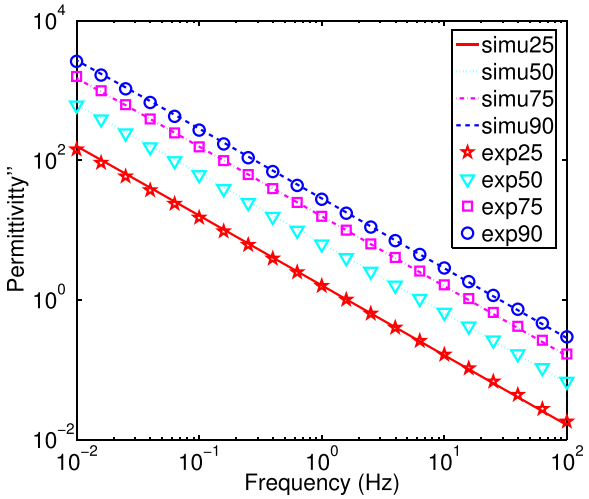


FIG. 7. The simulation and experimental result of the imaginary part of the complex permittivity of the heavily aged oil. Dashed line, dashed-dotted line, dotted line, and solid line are calculated by the means of the curve fitting at 90 °C, 75 °C, 50 °C, and 25 °C, respectively. Circular markers, square markers, triangular markers, and pentacle markers represent the observed value at 90 °C, 75 °C, 50 °C, and 25 °C, respectively.

where $\sigma_i$ is the conductivity contributed by the motion of the injected charge carriers. With this definition, Eq. (1) should be re-written as

$$n_+ = n_- = n_0 = (1-\alpha)\sigma/q(\mu_+ + \mu_-). \tag{45}$$

As seen from the experiment, the imaginary part of the complex permittivity $\varepsilon''(\omega)$ decreases with the frequency in a slope of approximately $-1$, which means that $\varepsilon''(\omega)$ is proportional to the angular frequency $1/\omega$. In our previous discussion (see Sec. II), if the second kind of charge carriers are unable to get to the opposite electrode in a full field cycle, $\varepsilon''(\omega)$ will be proportional to $1/\omega^2$. If the mobility of the second kind of charge carriers can travel to the opposite electrode in a full cycle at 100 Hz, there is always a linear relationship between $\varepsilon''(\omega)$ and $1/\omega$ in the frequency range that is studied in this paper, which is in a good agreement with the experimental result. Thus, the majority of the injected charge carriers should have a high mobility so that they can get to the opposite electrode in a cycle. The minimum mobility $\mu_{\min}$ can be calculated as

$$\mu_{\min} = \frac{\omega l}{2E} = \frac{100 \times 2 \times \pi \times 5 \times 10^{-4}}{4 \times 10^3} \approx 7.9 \times 10^{-5}(\mathrm{m^2/s/V}). \tag{46}$$

If $\mu_i > \mu_{\min}$, Eq. (42) can be simplified as

$$\begin{cases} \varepsilon'(\omega) = \dfrac{2I_{imag}l}{\varepsilon_0 \omega V_0 S} + \varepsilon_s \\ \varepsilon''(\omega) = \dfrac{2I_{real}l}{\varepsilon_0 \omega V_0 S} + \dfrac{q_i^0 \mu_i}{\omega \varepsilon_0}. \end{cases} \tag{47}$$

Thus, the following expression can be obtained by using Eqs. (20) and (47):

$$\sigma_i = \mu_i q_i^0. \tag{48}$$

Please note, the injected charge carriers that have a low mobility and are unable to reach the opposite electrode in a full cycle might still exist in mineral oil. Here, we assume the conductivity contributed by those slow injected charge carriers is $\sigma_{i-slow}$. As seen from Eq. (41), the dielectric loss that is brought by the motion of those slow injected charge carriers should always be equal or smaller than $\sigma_{i-slow}/\omega\varepsilon_0$. Therefore, if their density is negligible, the dielectric loss caused by the motion of these slow injected charge carriers can also be ignored.

The simulation follows the procedure discussed by Sawada.[25–29] In this paper, the complex permittivity is calculated in the same way as in his work by dividing the space

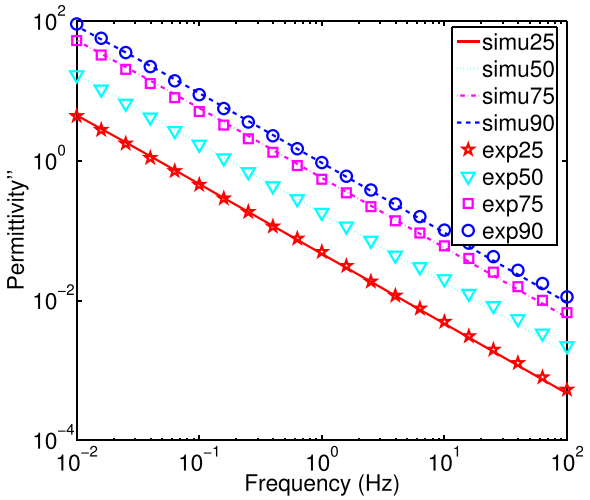


FIG. 6. The simulation and experimental result of the imaginary part of the complex permittivity of the lightly aged oil. Dashed line, dashed-dotted line, dotted line, and solid line are calculated by the means of the curve fitting at 90 °C, 75 °C, 50 °C, and 25 °C, respectively. Circular markers, square markers, triangular markers, and pentacle markers represent the observed value at 90 °C, 75 °C, 50 °C, and 25 °C, respectively.

between the two parallel electrodes into $N$ slabs. The initial condition is setting as the first kind of charge carriers is assumed to be evenly distributed in the bulk and there is no presence of the second type of charge carriers. After setting the initial condition, the calculation of the density of positive and negative charge carriers within a time interval $\Delta t = T/M$ is repeated for several cycles to get stationary values of $\varepsilon'(\omega)$ and $\varepsilon''(\omega)$ using Eq. (47). As pointed out by Sawada, the necessary cycles needed to acquire the stationary values of the complex permittivity increases with the frequency.[25–29] Therefore, a wait cycle number $K$, introduced by Sawada, which depends on the frequency to obtain the stationary values is set in our simulation.[25–29] It is worth noting that the approximation involved in this paper is valid only if the distance moved by a mobile charge in time $\Delta t$ is sufficiently smaller than the slab width $l/N$. This implies

$$\Delta t \ll \frac{l^2}{\mu V_0 N}. \tag{49}$$

The time interval and the number of slab should be set carefully so that Eq. (46) can be satisfied. The condition determined for the calculation in the steady state is summarized in Table I.

The distance between the two electrodes is 0.5 mm. The total conductivity is calculated from the imaginary part of the complex permittivity obtained experimentally using $\sigma = \omega\varepsilon_0\varepsilon''(\omega)$. The relative permittivity $\varepsilon_s$ is taken directly from the real part of the complex permittivity at 100 Hz measured in the experiments. The mobility of these charge carriers is assumed to be proportional to the reciprocal of the viscosity of the oil and the mobility of the charge carriers in the heavily aged oil is assumed to be $1 \times 10^{-9}\mathrm{m}^2/\mathrm{s/V}$. The viscosities of these mineral oils have been measured in our previous work.[43]

The simulation results of the complex permittivity of these three kinds of mineral oils with different aging times are illustrated in Figs. 2–7. Good fittings between observed and calculated values are achieved for the frequency-dependent curves of the complex permittivity. In all events, the real part of permittivity does not change much at high frequency (1 Hz–100 Hz) and increases significantly when the frequency goes lower and the imaginary part of complex permittivity decreases with the frequency with a slope that is close to $-1$ in log-log scale. It seems that if part of the charge carriers are injected from the electrode, both the real and imaginary parts of the complex permittivity can be fitted. The coefficient, $1-\alpha$, for three different types of mineral oils used in the simulation, is shown in Table II.

As seen from Table II, it seems when the oil is aged, the injected charge carriers will be the main charge carriers in the mineral oil. Also, a higher temperature can result in a smaller proportion of the first kind of the charge carriers and a larger amount of the second kind of charge carriers, which means that the injection can be enhanced by aging and high temperature.

TABLE I. Condition for the numerical calculation.

| Frequency (Hz) | Time coefficient $M$ | Slab number $N$ | Wait cycles $K$ |
|---|---|---|---|
| 100–1 | 10 000 | 50 | 5 |
| 1–0.01 | 100 000 | 50 | 3 |

TABLE II. The coefficient $1-\alpha$ for three different kinds of mineral oil.

| | 25 °C | 50 °C | 75 °C | 90 °C |
|---|---|---|---|---|
| Fresh oil | 0.8 | 0.45 | 0.4 | 0.38 |
| Lightly aged oil | 0.30 | 0.11 | 0.055 | 0.050 |
| Heavily aged oil | 0.105 | 0.095 | 0.090 | 0.080 |

A few words should be said on the interpretation of the charge injection theory in liquid. Equation (17) is valid only under the condition that two assumptions have satisfied. First, the injection equation was derived for the case where the electric field is not too intense, i.e., $\sqrt{e/16\pi\varepsilon_0\varepsilon_r E} \gg x_B$. According to Alj, $x_B \approx 0.3\mathrm{nm}$.[30] Thus, $\sqrt{e/16\pi\varepsilon_0\varepsilon_r E} \gg x_B$, when a field of $2 \times 10^3\,\mathrm{V/m}$ is applied. Second, the distortion of the internal field distribution is negligible and the electric field can be approximated by a homogeneous field. In our previous work, the electric field that is close to the electrodes and the electric field that is in the middle of the two metal electrodes are similar as the average field that is calculated from $E = V/l$ for all three kinds of mineral oils.[43] Besides, if the measurement is carried out under high electric field, more charge carriers will be created and the field distortion can be serious. Therefore, these assumptions are no longer valid under a high electric field. This model can only be used to explain the frequency response of mineral oil under a low electric field.

To sum up, the model with two kinds of charge carriers can fit the experimental data well. The ratio for the conductivity contributed by the injection current over the total conductivity $\alpha$ increases with the aging and temperature. This ratio may help us to gain a better understanding of electrical conduction in the mineral oil. However, this new space charge polarization model can still be improved. Apparently, these injected charge carriers can affect the internal field distribution. Thus, the real part of the complex permittivity of the mineral oil can also be affected by the charge injection. The nature of these injected charge carriers is still not clear.

## IV. CONCLUSION

The present work is concentrated on the analysis of dispersion of dielectric permittivity of mineral oil. Three types of mineral oil are tested. The conductivity of mineral oil increases with its aging time. The real part of the complex permittivity increases faster at a low frequency (below 1 Hz) when the oil is aged, whilst the imaginary part of the complex permittivity decreases with the frequency with a slope of $-1$ regardless of the conductivity.

The polarization induced by the injection current has been studied. When the mobility of these injected charge carriers is fast enough so that they can reach the opposite electrode, an ohmic conducting equation can be obtained. The new model that includes the contribution from charge

injection can fit the experimental data well. When the oil is aged, the charge injection takes a more important role in the electrical conduction. However, the polarization caused by injection is still not very clear and more research is needed.

## ACKNOWLEDGMENTS

The authors are grateful to National Grid UK for their financial support.

[1]F. Kremer and A. Schönhals, *Broadband Dielectric Spectroscopy* (Springer, 1998).
[2]A. A. S. Akmal, H. Borsi, and E. Gockenbach, IEEE Trans. Dielectr. Electr. Insul. **13**, 532 (2006).
[3]W. S. Zaengl, IEEE Electr. Insul. Mag. **19**, 5 (2003).
[4]R. Bartnikas, IEEE Trans. Dielectr. Electr. Insul. **16**, 1506 (2009).
[5]R. Z. Syunyaev and V. V. Likhatsky, Energy Fuels **24**, 2233 (2010).
[6]C. T. Dervos, C. D. Paraskevas, P. D. Skafidas, and N. Stefanou, IEEE Trans. Dielectr. Electr. Insul. **13**, 586 (2006).
[7]R. Bartnikas, *Engineering Dielectrics*, Electrical Insulating Liquids Vol. III (ASTM, 1994).
[8]T. K. Saha, IEEE Trans. Dielectr. Electr. Insul. **10**, 903 (2003).
[9]G. Jaffé, Ann. Phys. **408,**, 217 (1933).
[10]G. Jaffé, Phys. Rev. **85**, 354 (1952).
[11]H. C. Chang and G. Jaffé, J. Chem. Phys. **20**, 1071 (1952).
[12]G. Jaffe and C. Z. LeMay, J. Chem. Phys. **21**, 920 (1953).
[13]G. Jaffé and J. A. Rider, J. Chem. Phys. **20**, 1077 (1952).
[14]J. R. Macdonald, Phys. Rev. **92**, 4–17 (1953).
[15]R. Friauf, J. Chem. Phys. **22**, 1329 (1954).
[16]P. W. M. Jacobs and J. N. Maycock, J. Chem. Phys. **39**, 757 (1963).
[17]R. J. Klein, S. Zhang, S. Dou, B. H. Jones, R. H. Colby, and J. Runt, J. Chem. Phys. **124**, 144903 (2006).
[18]M. Iwamoto, J. Appl. Phys. **77**, 5314 (1995).
[19]F. C. M. Freire, G. Barbero, and M. Scalerandi, Phys. Rev. E **73**, 051202 (2006).
[20]A. D. Hollingsworth and D. A. Saville, J. Colloid Interface Sci. **257**, 65 (2003).
[21]R. Coelho, Rev. Phys. Appl. **18**, 137 (1983).
[22]R. Coelho, *Physics of Dielectrics for the Engineer* (Elsevier Pub. Co, New York 1979).
[23]D. G. Frood and T. J. Gallagher, J. Mol. Liq. **69**, 183 (1996).
[24]F. Stern and C. Weaver, J. Phys. C: Solid State Phys. **3**, 1736 (1970).
[25]A. Sawada, J. Appl. Phys. **100**, 074103 (2006).
[26]A. Sawada, J. Chem. Phys. **126**, 224515 (2007).
[27]A. Sawada, J. Chem. Phys. **129**, 064701 (2008).
[28]A. Sawada, J. Appl. Phys. **112**, 044104 (2012).
[29]A. Sawada, Phys. Rev. E **88**, 032406 (2013).
[30]A. Alj, A. Denat, J. P. Gosse, and B. Gosse, IEEE Trans. Electr. Insul. **EI-20**, 221 (1985).
[31]M. Nemamcha, J. P. Gosse, A. Denat, and B. Gosse, IEEE Trans. Electr. Insul. **EI-22**, 459 (1987).
[32]N. Felici and J. P. Gosse, Rev. Phys. Appl. **14**, 629 (1979).
[33]N. J. Felici, J. Electrost. **12**, 165 (1982).
[34]A. Denat, B. Gosse, and J. P. Gosse, J. Electrost. **11**, 179 (1982).
[35]A. Denat, B. Gosse, and J. P. Gosse, J. Electrost. **12**, 197 (1982).
[36]A. Denat, B. Gosse, and J. P. Gosse, J. Electrost. **7**, 205 (1979).
[37]J. C. Lacroix and P. Atten, J. Electrost. **5**, 453 (1978).
[38]N. Felici, IEEE Trans. Electr. Insul. **EI-20**, 233 (1985).
[39]C. Brosseau, J. Appl. Phys. **69**, 891 (1991).
[40]F. Pontiga and A. Castellanos, IEEE Trans. Dielectr. Electr. Insul. **3**, 792 (1996).
[41]F. Pontiga and A. Castellanos, IEEE Trans. Dielectr. Electr. Insul. **32**, 816 (1996).
[42]L. Onsager, J. Chem. Phys. **2**, 599 (1934).
[43]Y. Zhou, M. Hao, G. Chen, G. Wilson, and P. Jarman, in *Proc. IEEE CEIDP*, Shenzhen, China, October 2013, Vol. 1, p. 587.
[44]B. Gänger and G. Maier, Brown Boveri Review **10**, 525 (1969).
[45]A. Castellanos, *Electrohydrodynamics* (Springer, New York, 1998).
[46]P. Langevin, Ann. Chim. Phys. **28**, 433 (1903).